

Supplementary Information

A peptide derived from the core β -sheet region of TIRAP decoys TLR4 and reduces inflammatory and autoimmune symptoms in murine models

Asma Achek¹, Hyuk-Kwon Kwon², Mahesh Chandra Patra¹, Masaud Shah¹, Riwon Hong³, Wang Hee Lee¹, Wook-Young Baek⁴, Yang Seon Choi¹, Gi-Young Kim¹, Thuong L.H Pham¹, Chang-Hee Suh⁴, Wook Kim¹, Dae-Hyun Hahm³, Sangdun Choi^{1,*}

¹Department of Molecular Science and Technology, Ajou University, Suwon 16499, Korea

²Department of Orthopaedics and Rehabilitation, Yale School of Medicine, New Haven, CT 06510, USA

³Department of Physiology, School of Medicine, Kyung Hee University, Seoul 02447, Korea

⁴Department of Rheumatology, Ajou University School of Medicine, Suwon 16499, Korea

*Correspondence: Sangdun Choi

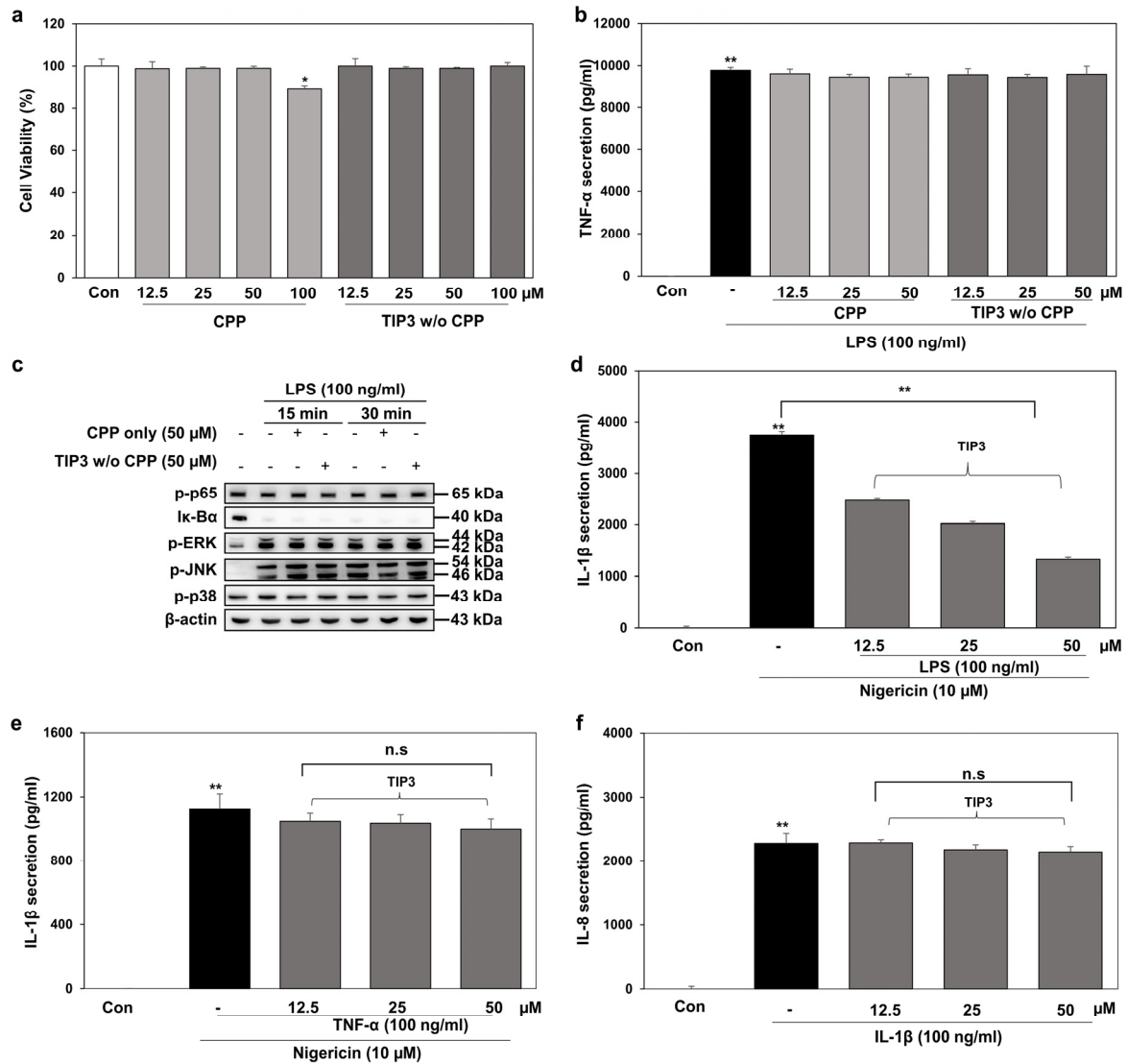
Department of Molecular Science and Technology, Ajou University, Suwon 16499, Korea

Phone: +82 31-219-2600

Fax: +82 31-219-1615

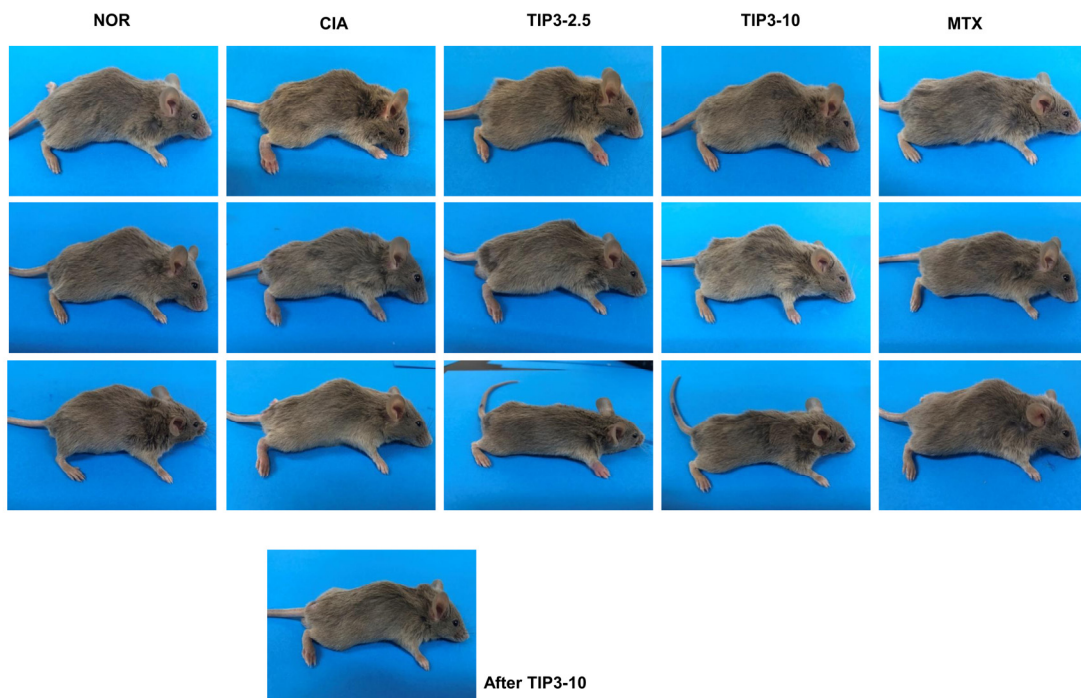
E-mail: sangdunchoi@ajou.ac.kr

Supplementary Figures

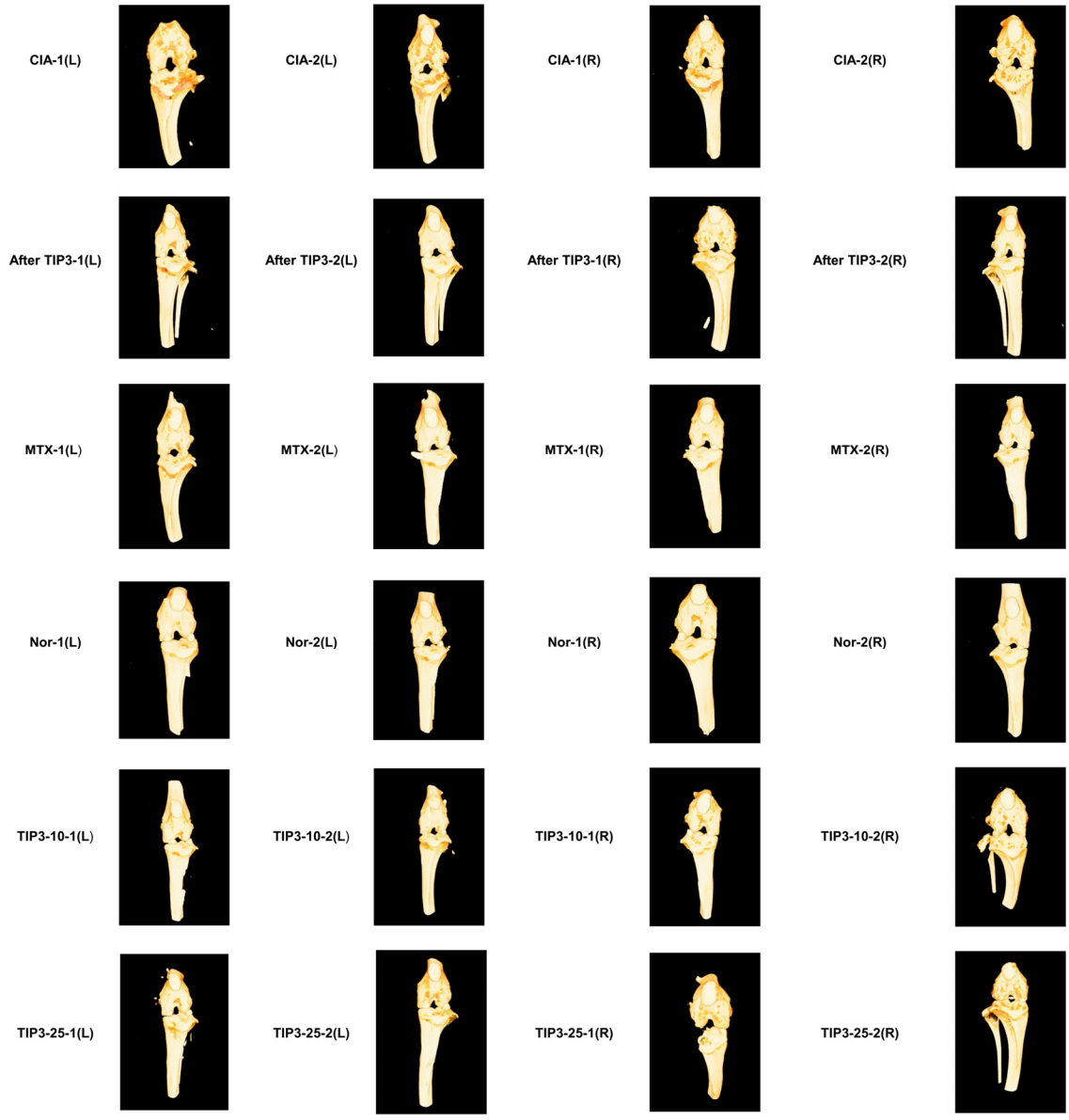


Supp Fig. 1. *In vitro* Supporting data regarding TIP3 experiments. (a) Cell viability analysis for free penetratin CPP- and unconjugated TIP3- (referred to as TIP3 w/o CPP) treatment in RAW264.7 cells. Both tested peptides did not manifest any inhibitory effect on LPS-induced **(b)** TNF- α secretion on RAW264.7 cells and did not hinder the **(c)** protein expression levels of p-p65, I κ -B α , p-ERK, p-JNK, and p-p38. β -actin served as a loading control. **(d, e)** The modulatory effect of TIP3 on NLRP3 inflammasome activation was evaluated by measuring the secretion level of IL-1 β in THP-1 following the priming with **(d)** LPS and **(e)** TNF- α . **(f)** TIP3 did not display any inhibitory effect on the IL1R-mediated IL-8 secretion level, following the treatment of THP-1 cells with IL-1 β . The data shown represent

at least three independent experiments ($n \geq 3$), and bars denote mean \pm SEM (*P < 0.05, **P < 0.01).



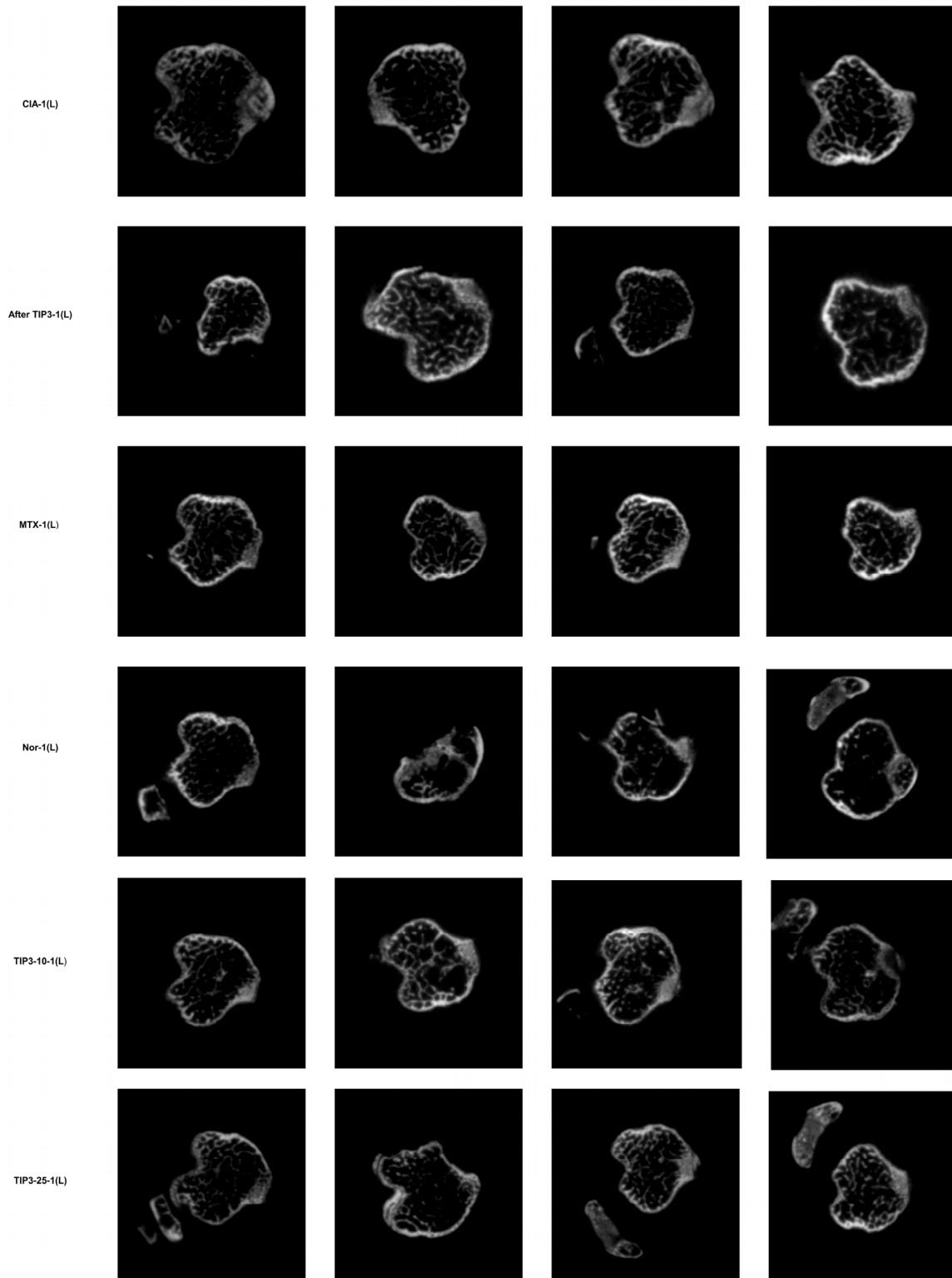
Supp Fig. 2. Representative photographs of the mice taken on day 45.



Supp Fig. 3. The 3D images of the knee joints captured by Micro-CT to estimate the joint corrosion and cartilage loss.



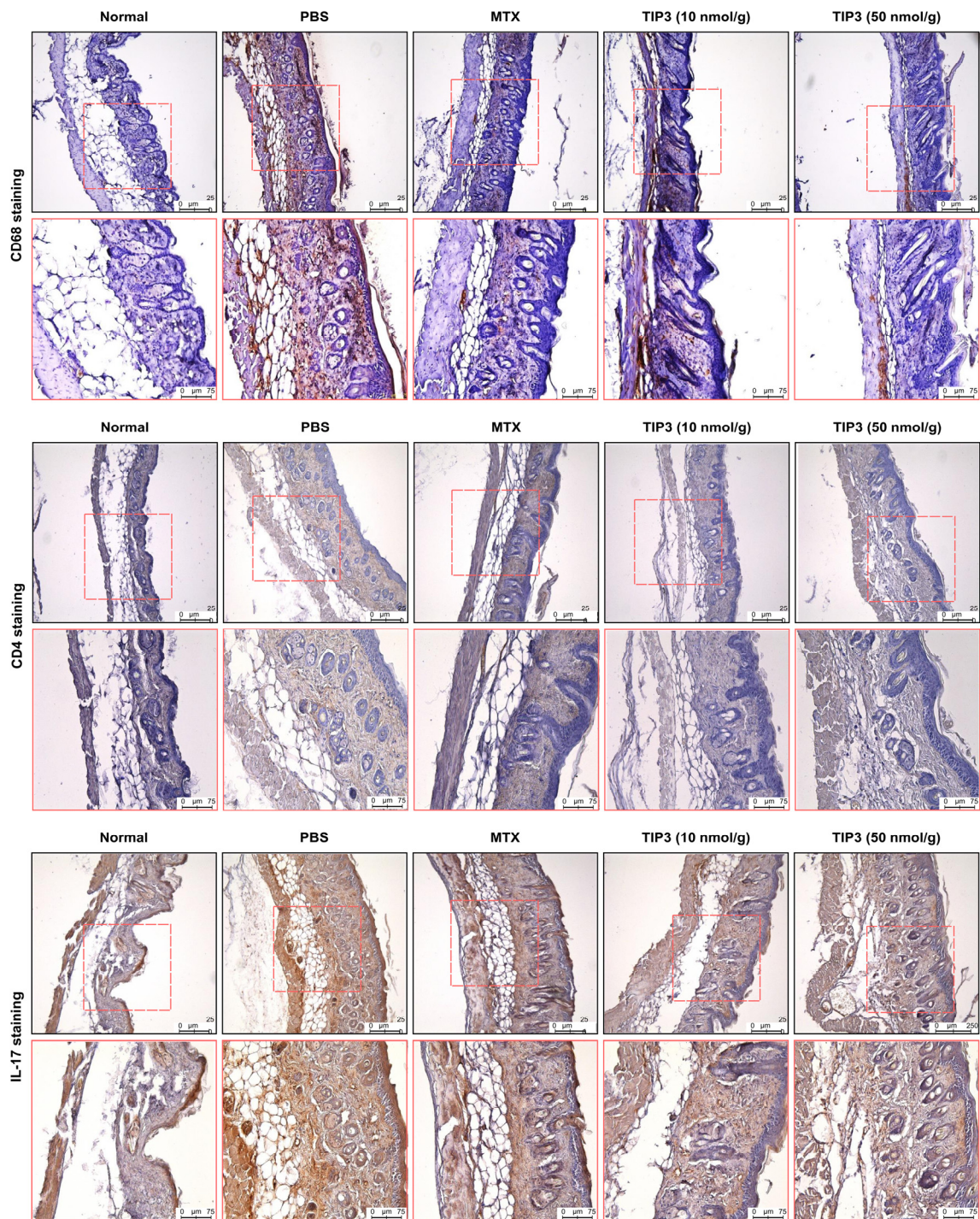
Supp Fig. 4. Representative 2D images of trabecular bone corresponding to the sagittal section at the top of a tibia as measured by Micro-CT.



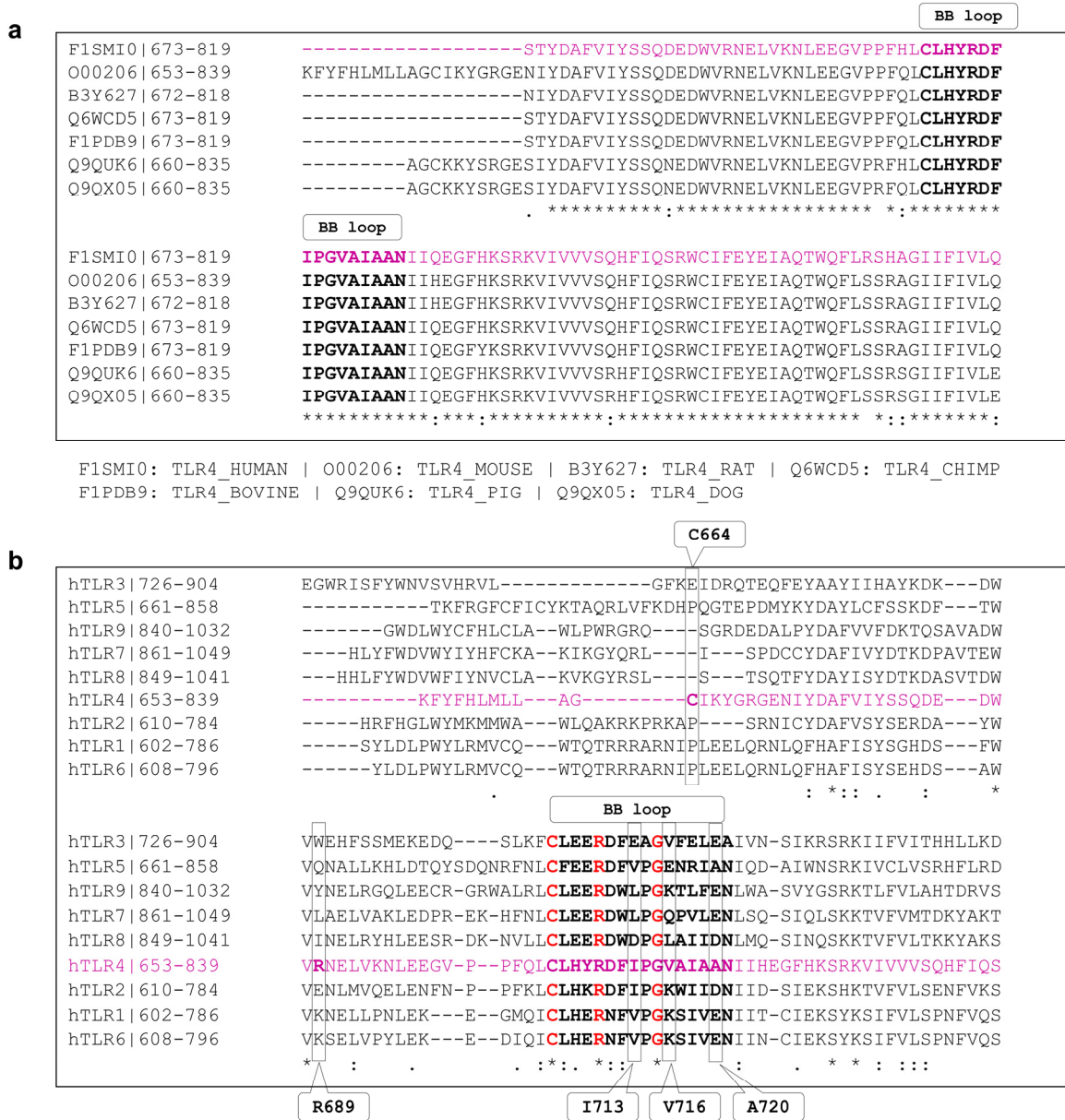
Supp Fig. 5. Cortical bones corresponding to the horizontal section in the middle of a tibia as measured by Micro-CT.

Supp Table 1. The list of the primers used in this study.

Target gene	Primer	Sequence (5'–3')
Interleukin 1 beta	IL-1 β (F)	GAAAGCTCTCCACCTCAATG
	IL-1 β (R)	GCCGTCTTTCATTACACAGG
Interleukin 6	IL-6 (F)	CCAGAGATACAAAGAAATGATGG
	IL-6 (R)	ACTCCAGAAGACCAGAGGAAA
Chemokine (C-X-C motif) Ligand 10	CXCL-10 (F)	GCCGTCATTTTCTGCCTCAT
	CXCL-10 (R)	GCTTCCCTATGGCCCTCATT
Interferon beta	IFN- β (F)	CGTGGGAGATGTCCTCAACT
	IFN- β (R)	AGATCTCTGCTCGGACCACC
Tumor Necrosis Factor alpha	TNF- α (F)	CACCACCATCAAGGACTCAA
	TNF- α (R)	AGGCAACCTGACCACTCTCC
Beta actin	β -actin (F)	GTTACAGGAAGTCCCTCACCC
	β -actin (R)	CAGACCTGGGCCATTTCAGAAA
Glyceraldehyde-3-phosphate dehydrogenase	GAPDH (F)	CATGTAGGCCATGAGGTCCACCAC
	GAPDH (R)	TGA AGC AGG CAT CTG AGGG



Supp Fig. 6. TIP3 alleviates the hyperproliferative state of the skin in the mouse model of psoriasis. Immunohistochemical analysis of the back skin lesions in each group as evaluated by immunohistochemical analysis. The scale bars are as follows: 250 μm for low-magnification (upper images) and 75 μm for high-magnification (bottom images).



Supp Fig. 7. Sequence alignment between TIR domains of human TLRs. (a) Alignment of TLR4 TIR domain sequences of selected species. TLR4 sequence is colored magenta and the BB loop motif is highlighted with bold fonts. **(b)** Alignment of TIR domain sequences of human TLRs. TLR4 sequence is magenta colored and BB loop is shown in bold fonts. The conserved residues in the BB loop of different TLRs are colored red. The residues identified in the docking analysis to interact with TIP3 is shown in black boxes. Identical residues are indicated by ‘*’, conservative substitutions and semiconservative substitutions are marked with ‘:’ and ‘.’, respectively.

Supplementary Method

In silico analyses

1. Construction of the three-dimensional (3D) model of TIP3

TIP3 was conjugated with penetratin, a cell-penetrating peptide (CPP), to facilitate membrane insertion and translocation. Note that TIP3 refers to the TIRAP-derived bioactive segment plus the CPP unless stated otherwise. The 3D model of CPP-conjugated TIP3 was manually constructed on the basis of a predicted secondary structure (PSIPRED)¹ in Discovery Studio (DS) Visualizer (Dassault Systèmes BIOVIA, San Diego, CA, USA). Energy minimisation and molecular dynamics (MD) simulation of the peptide were carried out over a dipalmitoyl phosphatidylcholine bilayer to model a reasonable side chain tertiary geometry. The peptide was positioned 10 Å above the bilayer surface and MD simulation was performed in GROMACS 5.0.7 software².

2. MD simulation parameters and protocol

The MD simulation of modelled TIP3 was carried out over a pre-equilibrated dipalmitoyl phosphatidylcholine bilayer consisting of 288 phospholipids. A modified force field having GROMOS96 54A7 and Berger lipid parameters was chosen for this task. The orientation and placement of the peptide on the membrane were accomplished in VMD 1.9.1³. Simple point charge water molecules and a physiological concentration (0.15 M) of counterions (Na⁺/Cl⁻) were added for charge neutralisation. Steepest descent energy minimisation was conducted to remove steric conflicts between atoms. MD simulation was first performed with the NVT ensemble and then with NPT ensemble for 100 ps. The production run was carried out for 100 ns via the NPT ensemble with no restraints on the backbone heavy atoms. Short-range (Lennard Jones) interactions were calculated with a 12 Å cut-off distance via the Verlet scheme, and long-range (Coulomb) interactions were computed by the particle mesh Ewald algorithm. The periodic boundary condition was applied to the simulation system. Temperature and pressure

couplings were performed with Nose-Hoover at 300 K and the Parrinello-Rahman algorithms at 1 bar, respectively. The linear-constraints-solver algorithm was applied to constraints all bonds involving hydrogen atoms and structural snapshots were taken every 2 ps.

3. Protein-protein docking procedure

The interaction of TIP3 with the TLR4 TIR domain was calculated via protein–protein docking on HADDOCK 2.2 web server⁴. The final snapshot of the TIP3 MD trajectory was docked to the TIR domain of a recently reported TLR4 model⁵. The highest-scoring docked complex from the largest cluster was chosen for detailed structural analysis after thorough energy minimisation.

References:

1. Jones DT. Protein secondary structure prediction based on position-specific scoring matrices. *J Mol Biol* 1999; **292**(2): 195-202.
2. Van Der Spoel D, Lindahl E, Hess B, Groenhof G, Mark AE, Berendsen HJ. GROMACS: fast, flexible, and free. *J Comput Chem* 2005; **26**(16): 1701-18.
3. Humphrey W, Dalke A, Schulten K. VMD: visual molecular dynamics. *J Mol Graph* 1996; **14**(1): 33-8, 27-8.
4. van Zundert GCP, Rodrigues J, Trellet M, et al. The HADDOCK2.2 Web Server: User-Friendly Integrative Modeling of Biomolecular Complexes. *J Mol Biol* 2016; **428**(4): 720-5.
5. Patra MC, Kwon HK, Batool M, Choi S. Computational Insight Into the Structural Organization of Full-Length Toll-Like Receptor 4 Dimer in a Model Phospholipid Bilayer. *Front Immunol* 2018; **9**: 489.